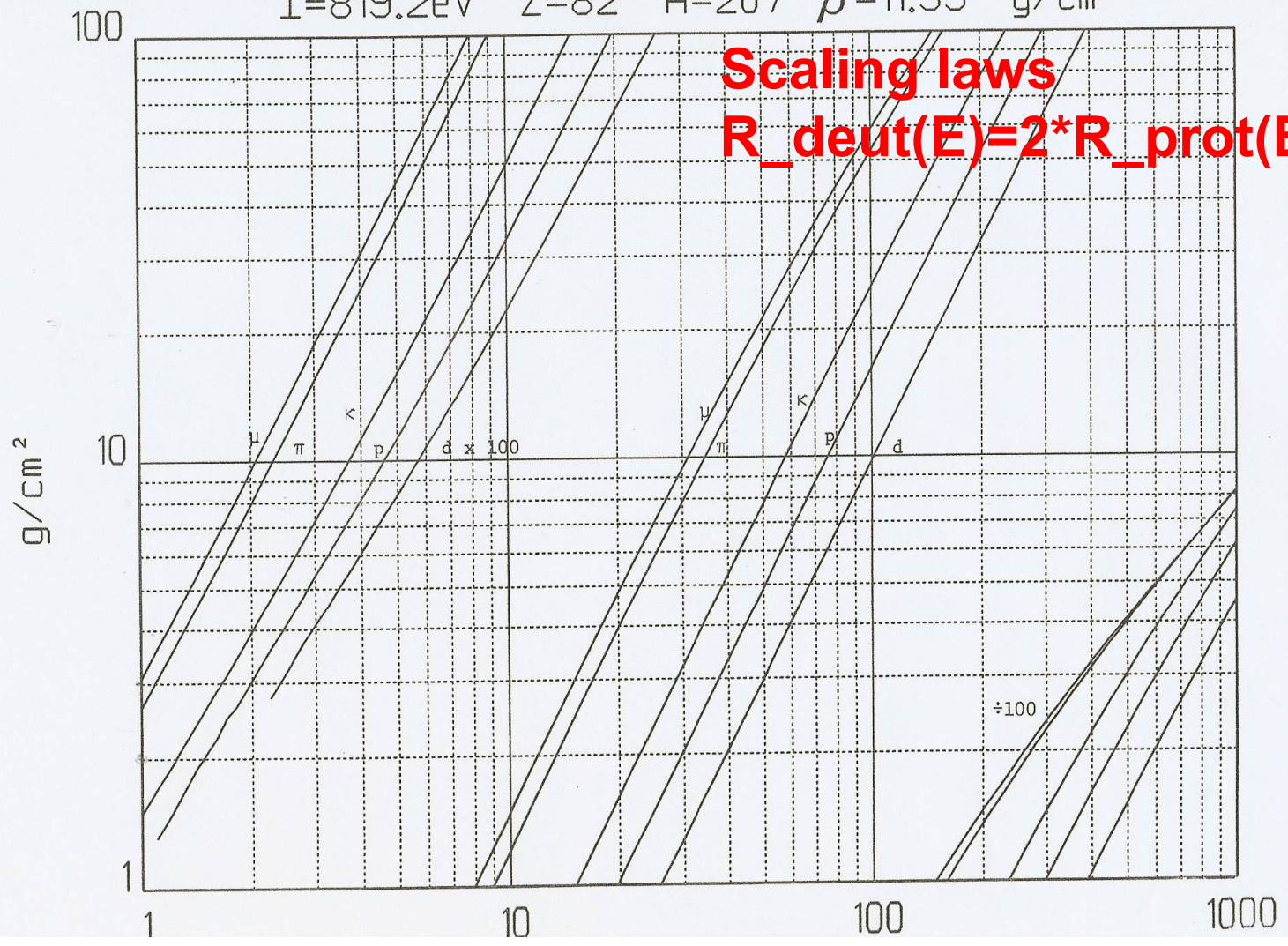
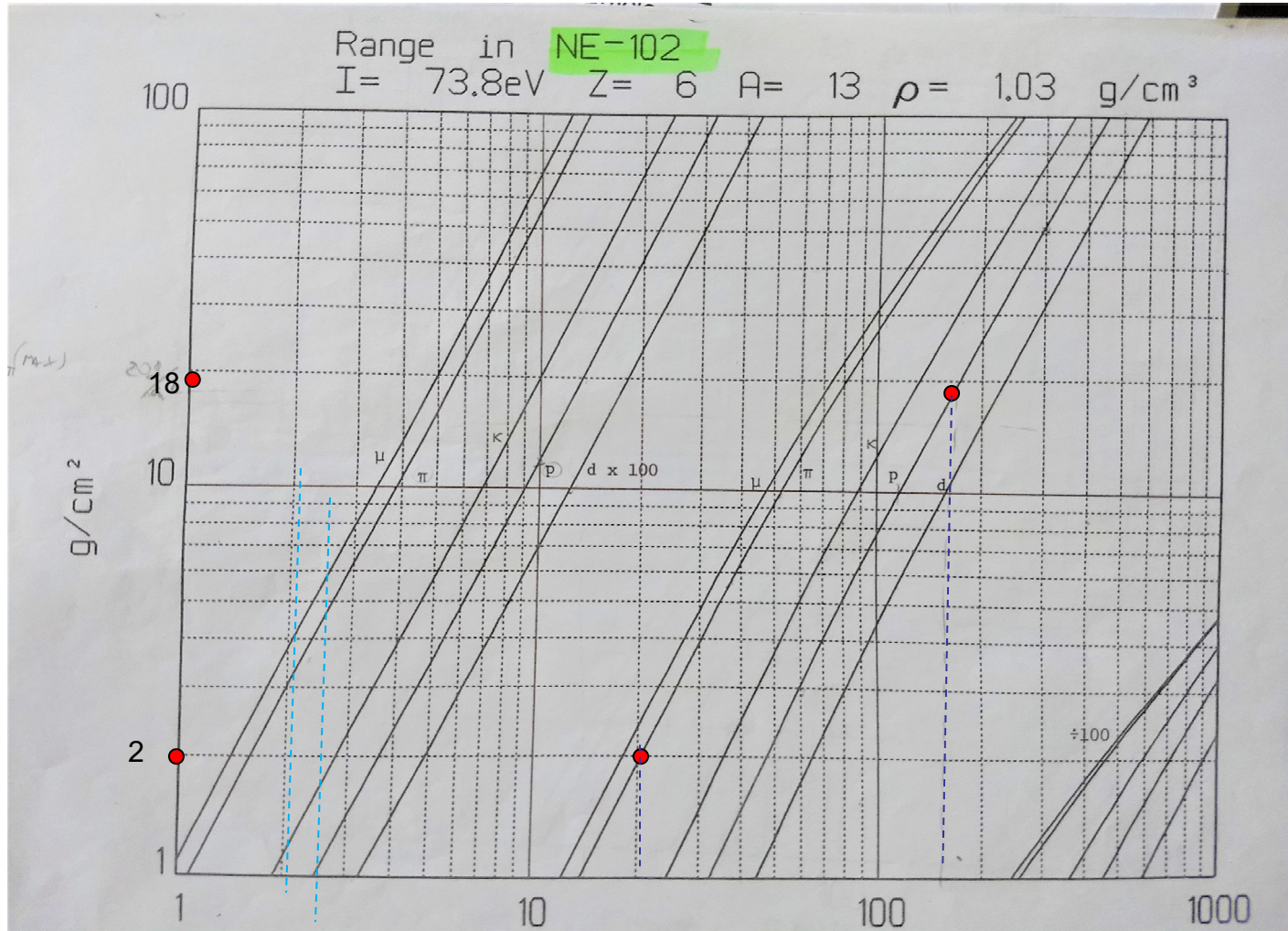


Range in Lead (Pb)
I=819.2eV Z=82 A=207 $\rho=11.35 \text{ g/cm}^3$

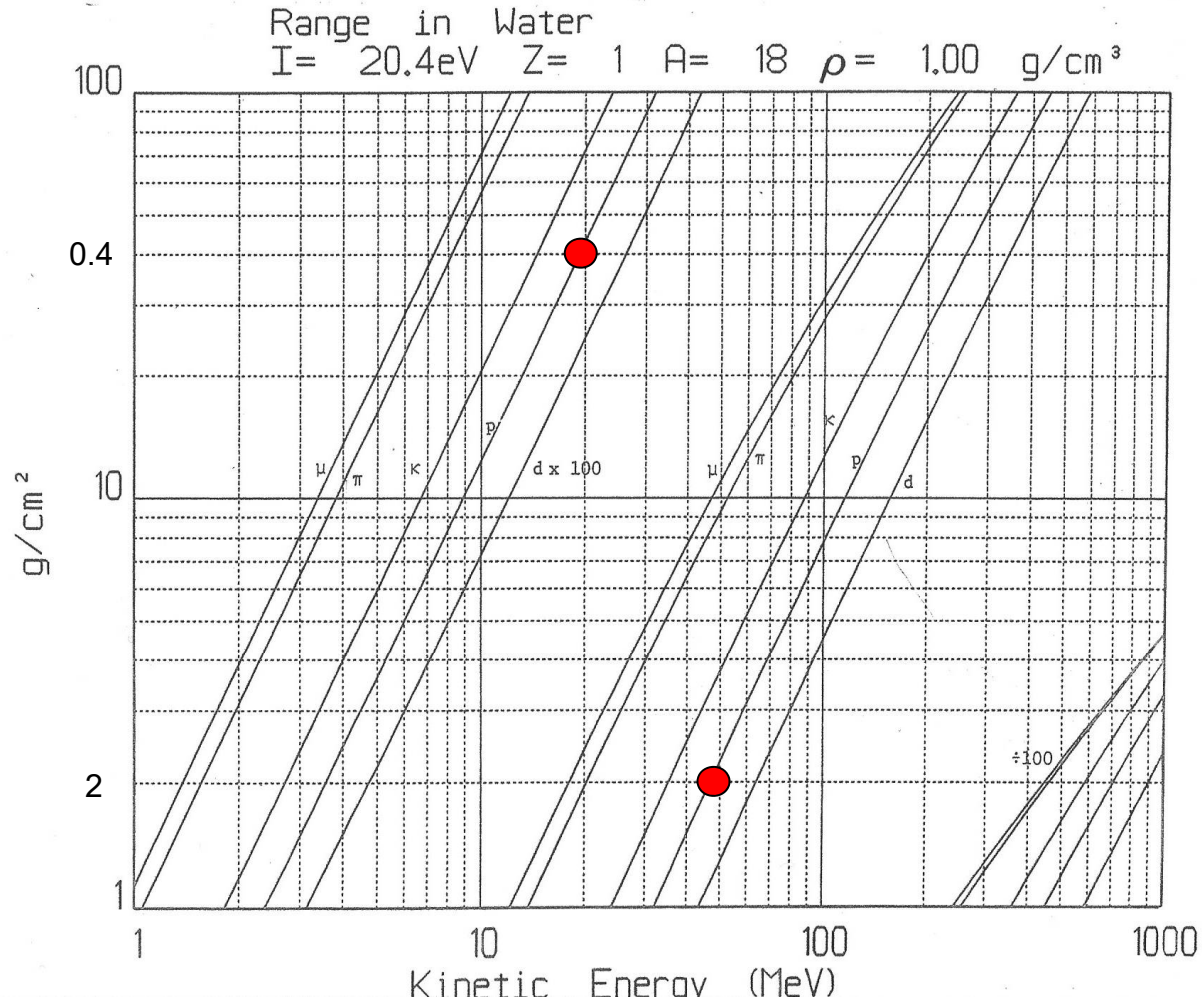


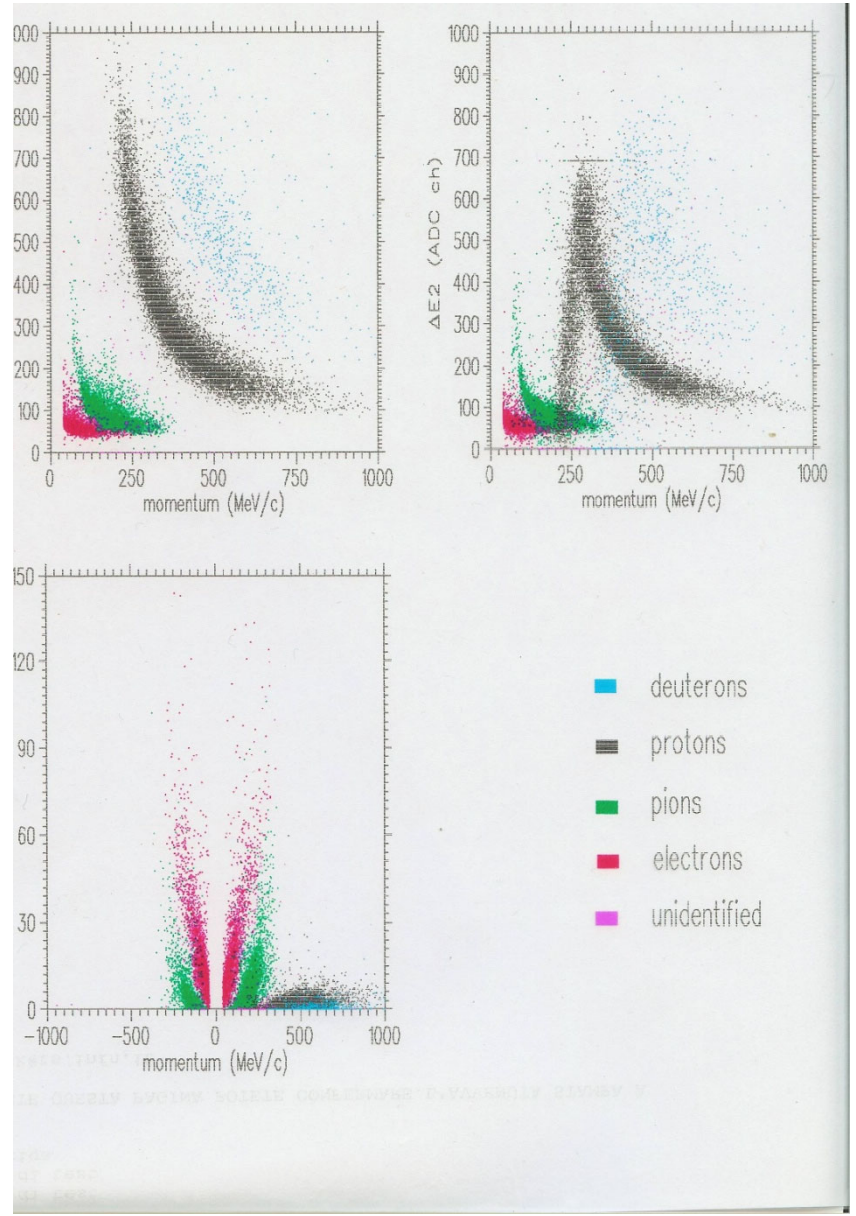
Mass discrimination also possible by making RANGE measurements

See exercise n. 7 on range discrimination

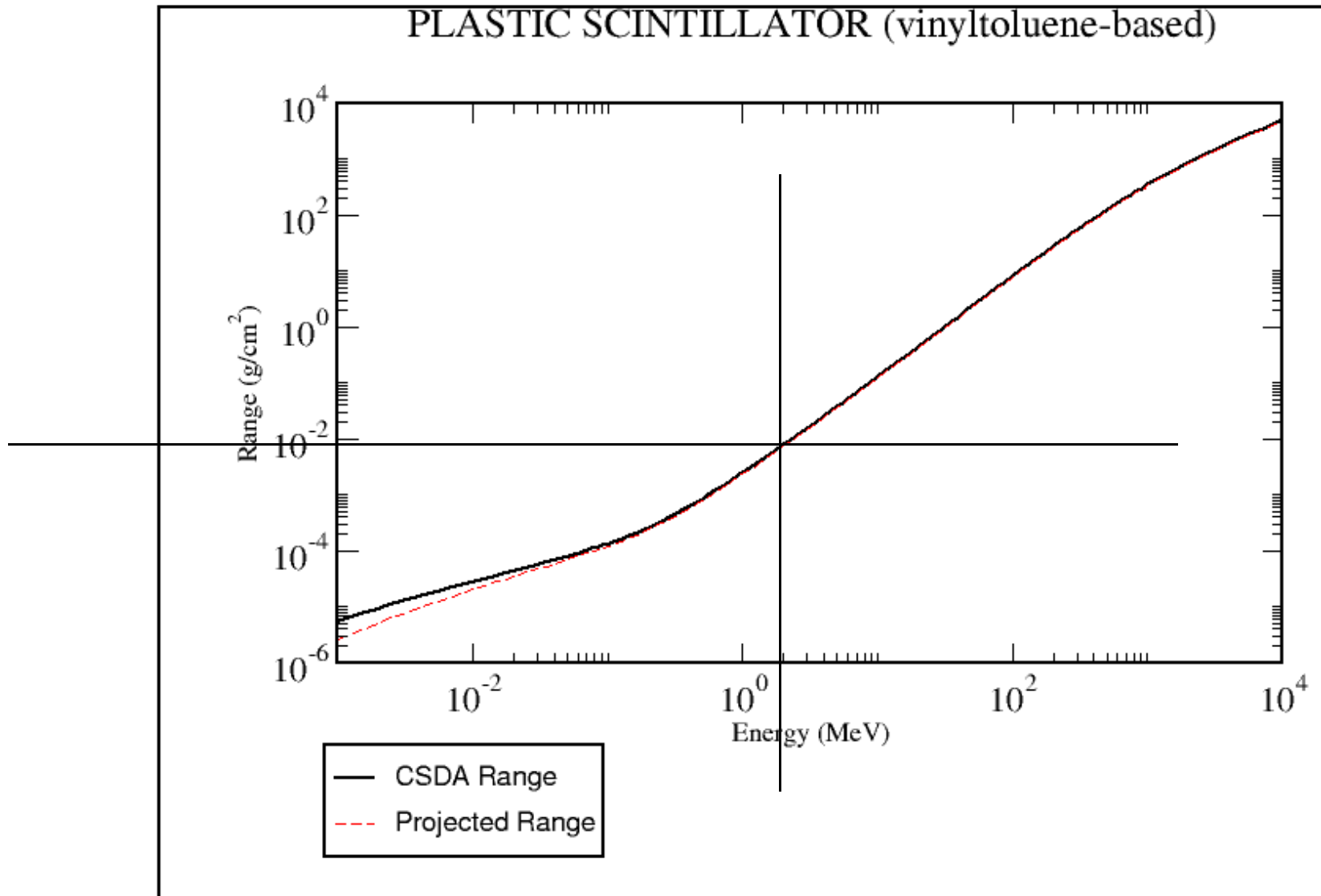


Exercise on energy loss inside/outside tumor

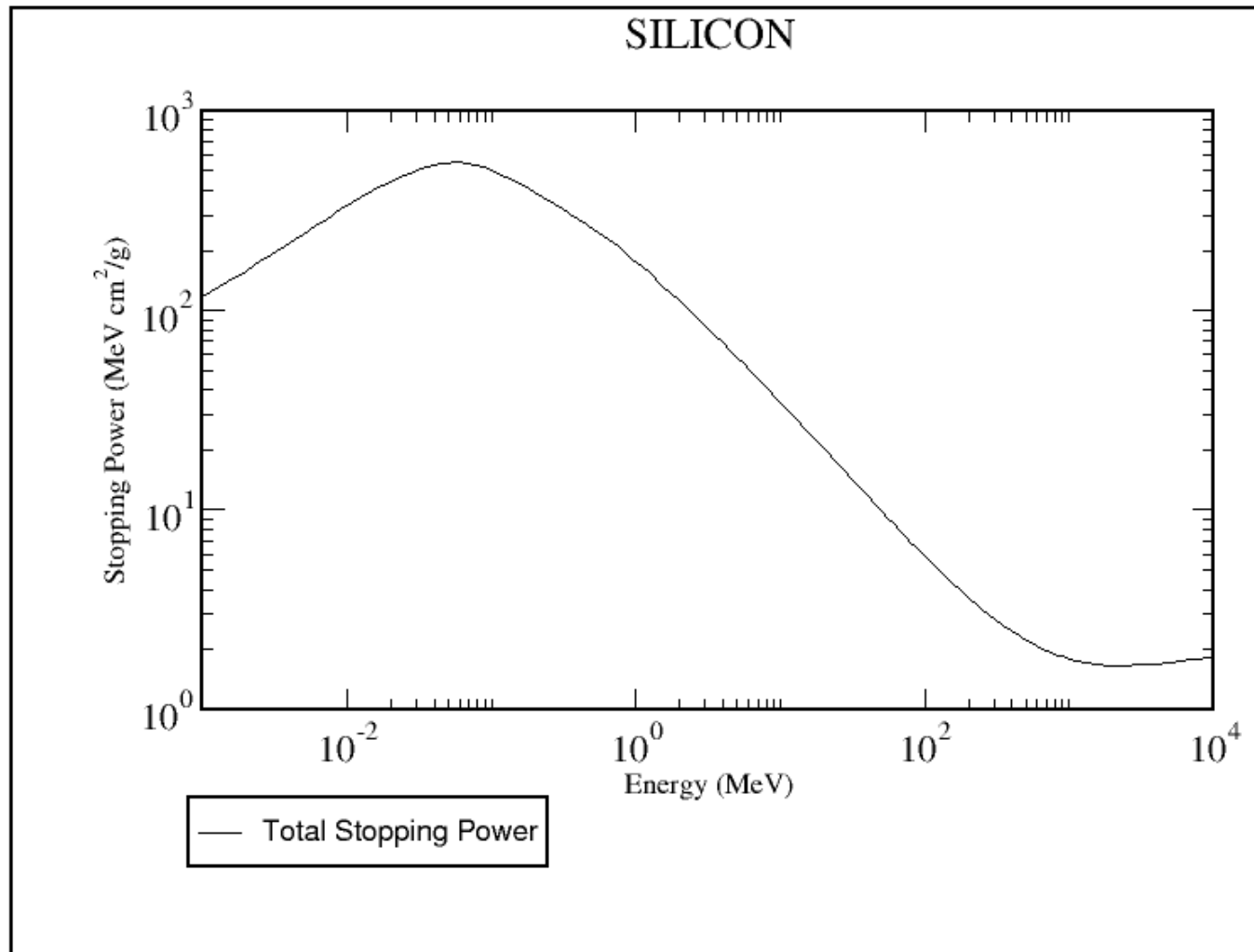




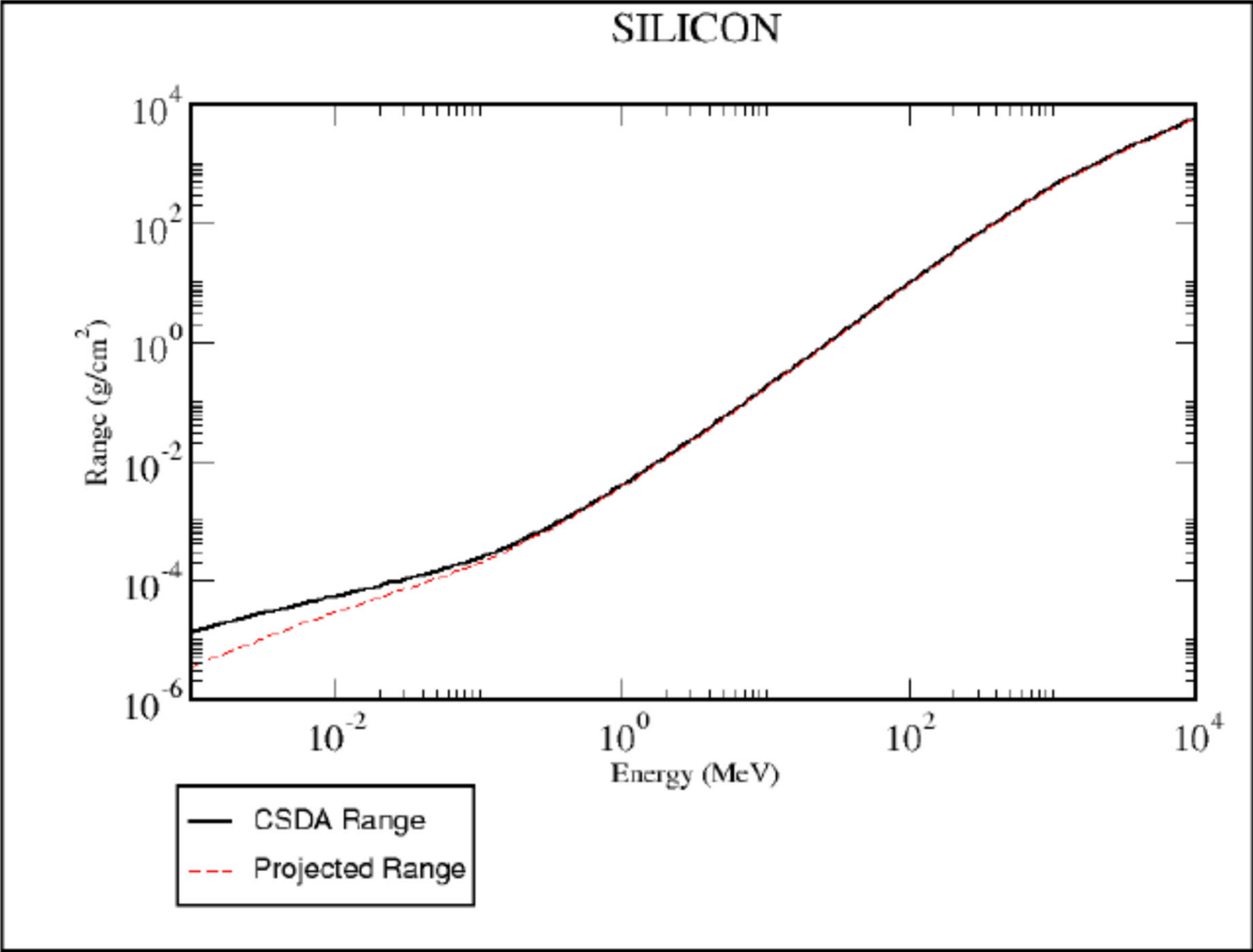
Range for protons in pl. scint



Stopping power for protons in silicon

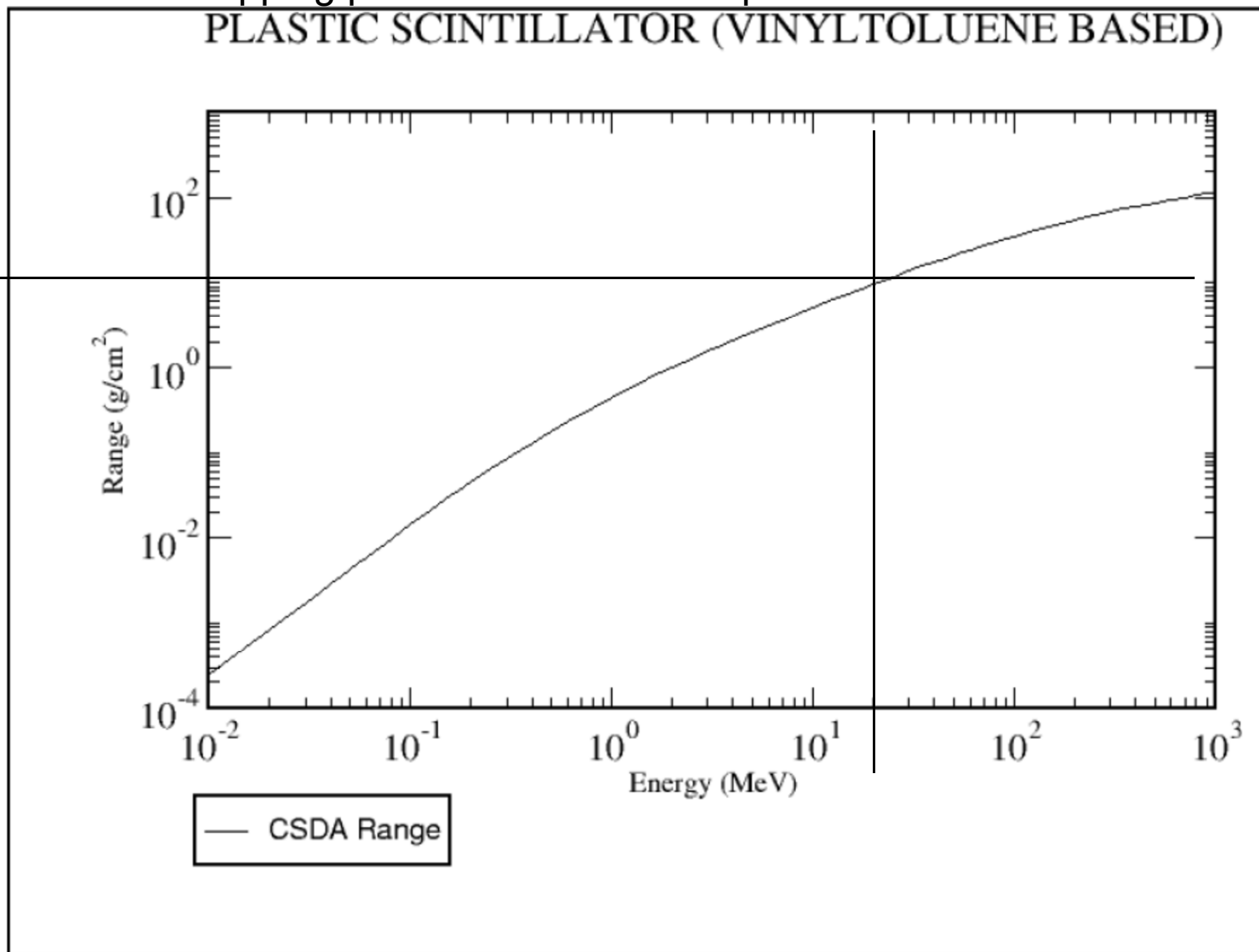


Range for protons in silicon



Stopping power for electrons in pl. scint

PLASTIC SCINTILLATOR (VINYL TOLUENE BASED)



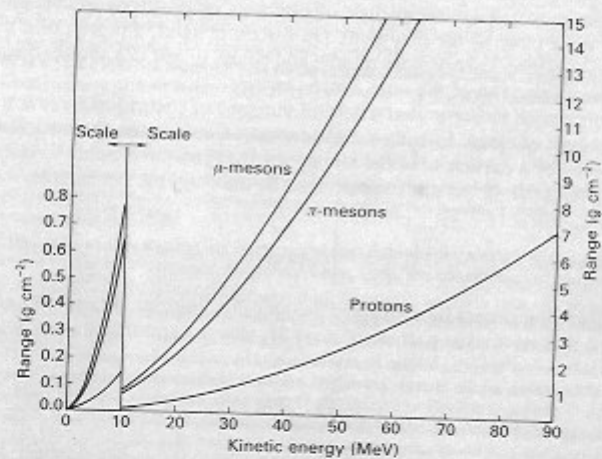


Fig. 11.3 The range-kinetic energy curves for protons, π -mesons and μ -mesons in carbon. Equation (11.1) tells us that at low energies the rate of energy loss is varying inversely as the velocity squared and therefore every increment in incident energy requires a disproportionate increase in range to remove that increase in energy; thus for all particles the range increases faster than linearly with the incident kinetic energy. In addition, Figure 11.2 shows that for the same kinetic energy lighter particles suffer less energy loss and therefore have greater ranges. Thus the features of this figure can be predicted from the properties of the stopping power.

the two particles. Light electrons of a given velocity have low momentum and are easily scattered or badly suffer the effect of multiple scattering, both of which cause an increasing deviation from a straight track, and that means that the track length has a projection on the original electron direction which is shorter or much shorter than the track length (see Fig. 11.5). For α -particles of the same velocity, the momentum is much greater and the track suffers much less deviation and the projected track length is in most cases only slightly less

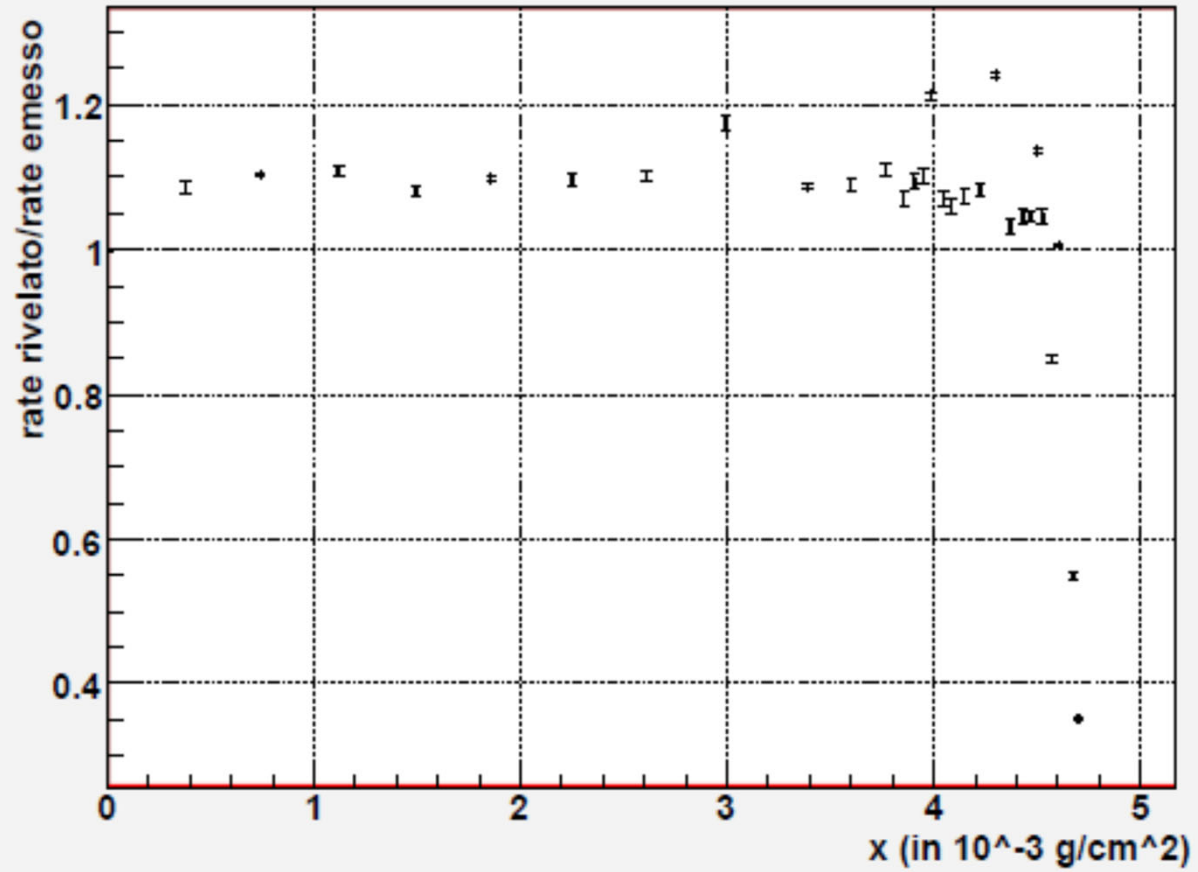
Scintillations per minute
70
60
50
40
30
20
10

Thickness:

Fig. 11.4 The trans hydrogen gas at 15°C other curves by visu from a source react scintillations per min energy the chance of the loss of energy fluctuation on the α -particles travel the until a thickness of definition of range is and the fact that the length (Fig. 11.5). If range could be cut scintillations become point where the curv Fig. 6.6 is a cloud unique range and sr

angle deviation is ap deviation, θ_0 ; it is th

CURVA DI RANGE



Curva di range sperimentale.

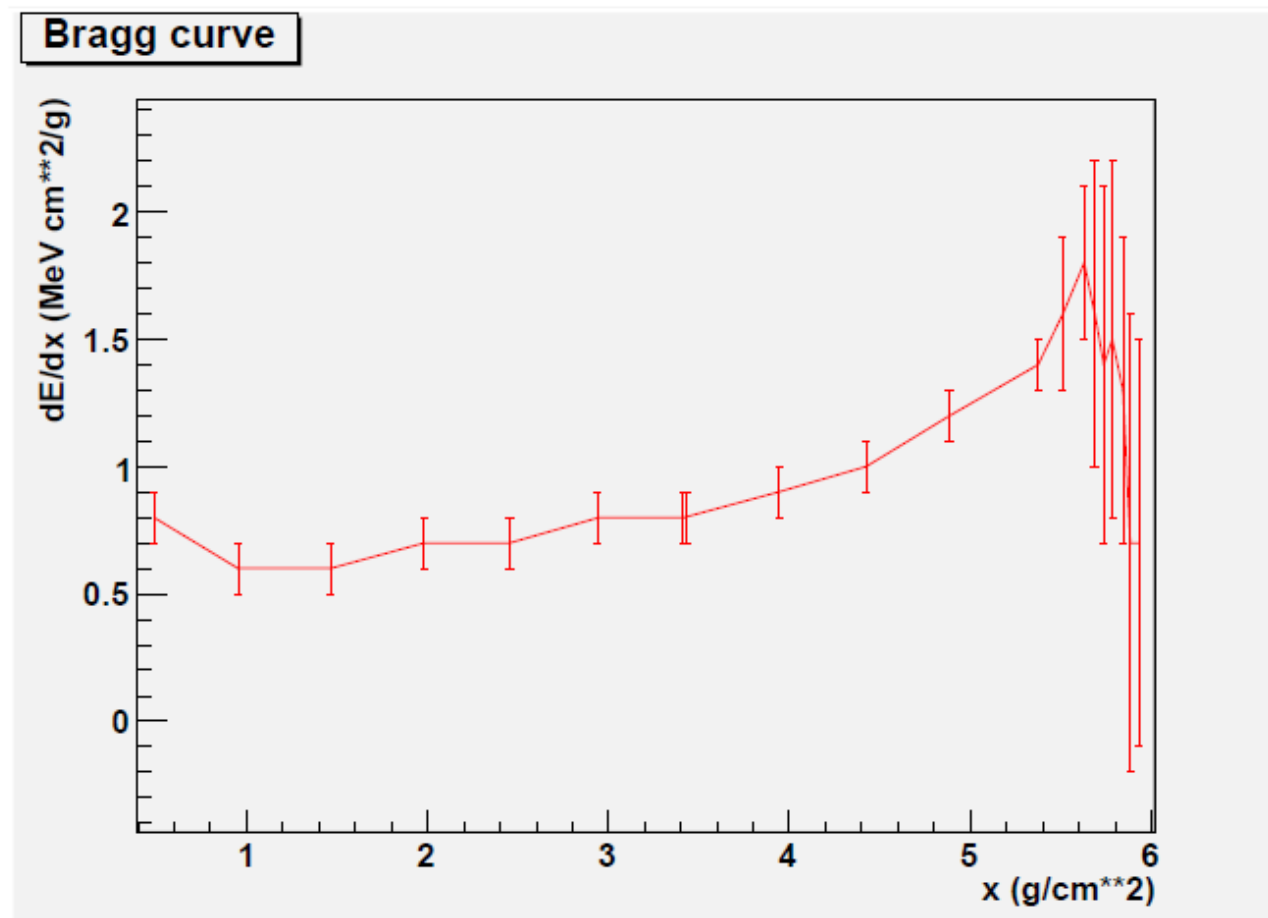
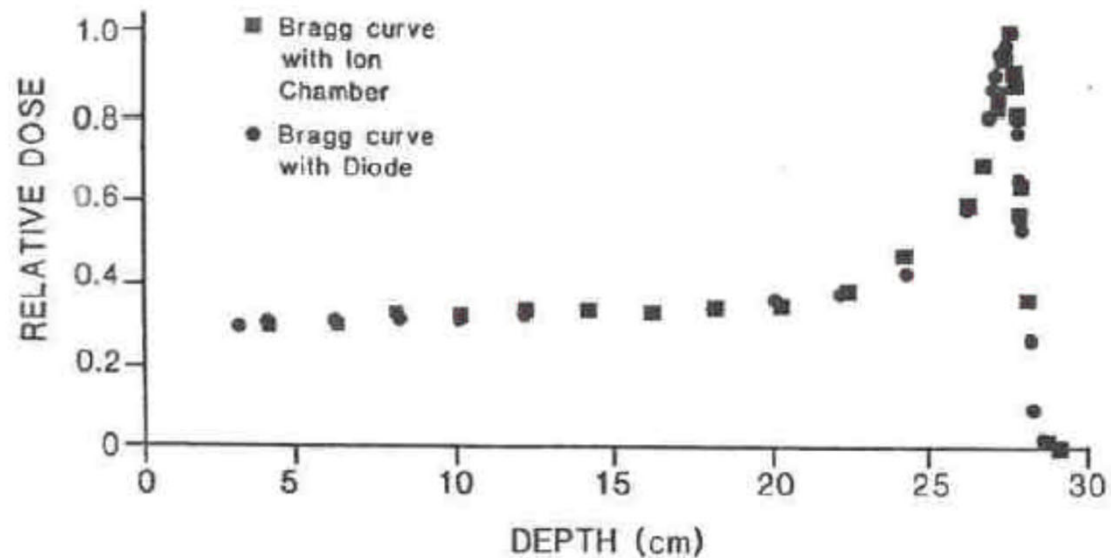


Figura 8: Grafico della curva di Bragg.

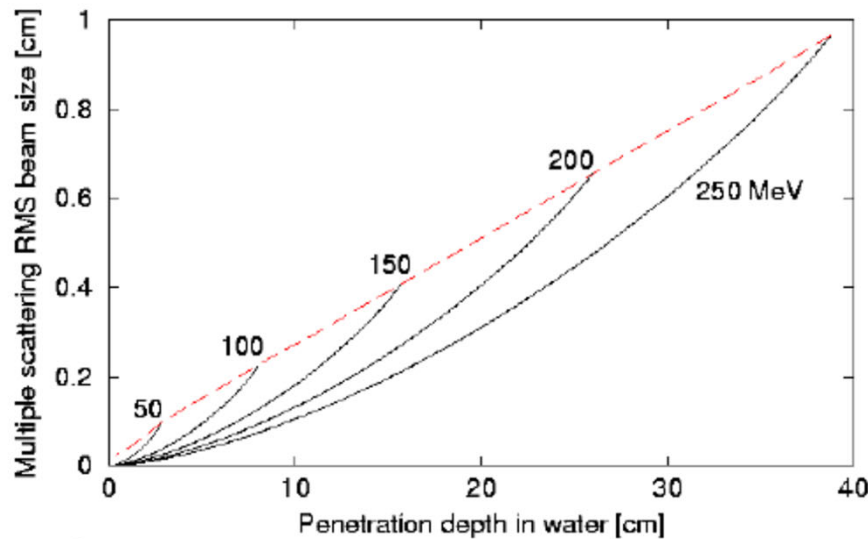
235 MeV Proton Bragg Curve

Loma Linda University Medical Center



- Suitable for 1.5 cm diameter tumor.
- Skin dose ~30% of maximum dose.

Coutrakon *et al*, Med. Phys. 1991. 18:1093-1099.

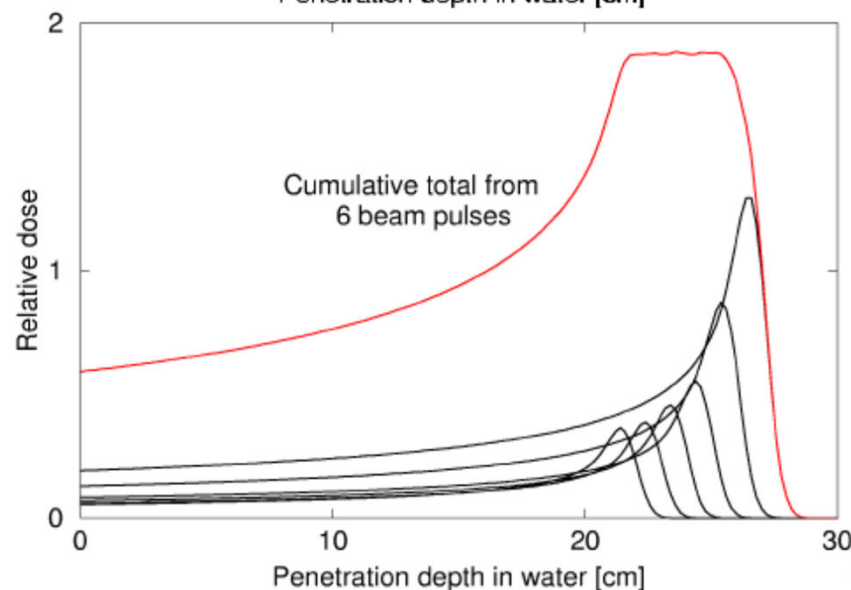


A perfect
monochromatic
proton beam, with
zero initial emittance:

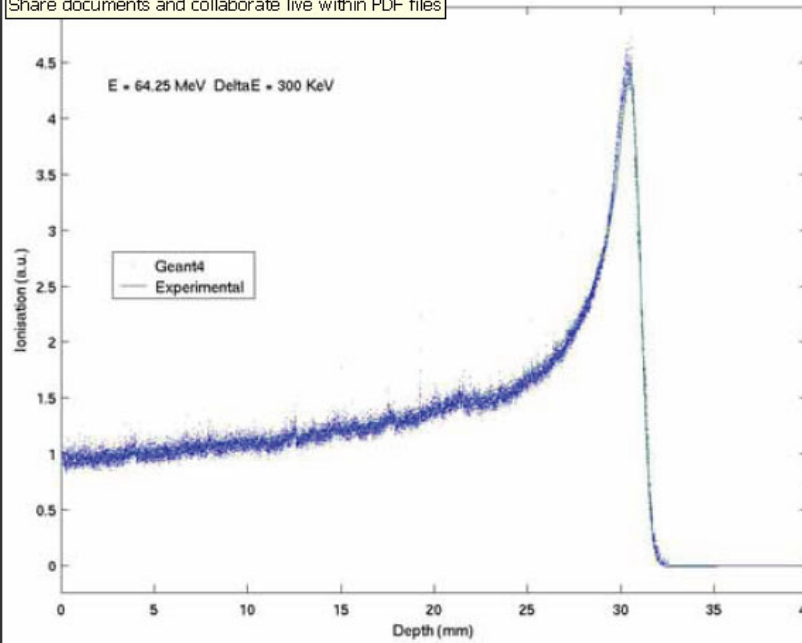
TOP spreads out
transversely

BOTTOM acquires
an energy spread that
blurs the Bragg peak

Steer the beam and
modulate its energy
to “paint” the tumor!



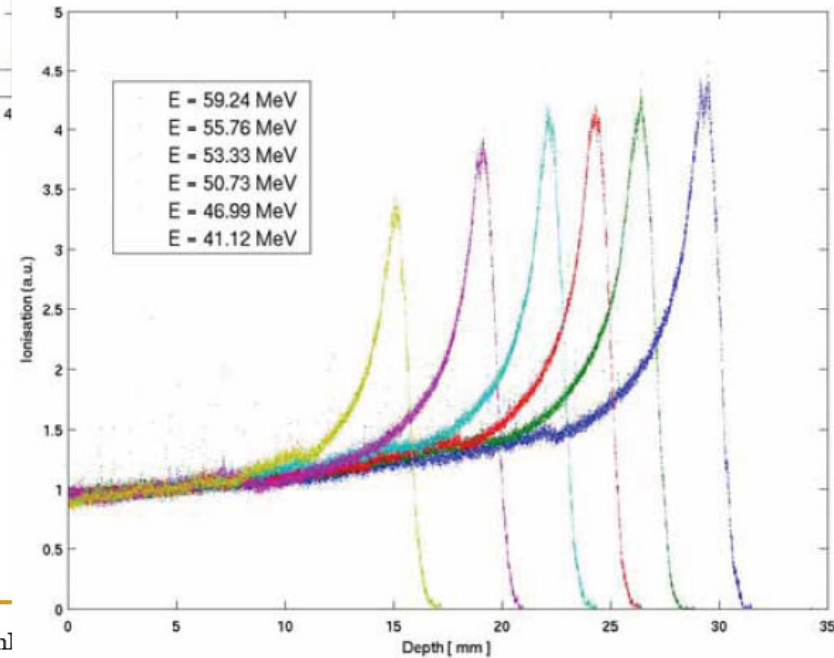
Share documents and collaborate live within PDF files



Physic models: comparison vs experimental data

Low energy libraries and hadronic physics

Bragg peaks at different energies



giovedì 24 maggio 2007

G.A.P. Cirrone Phl
Laboratori Nazionali del Sud CATANIA

25

Energy straggling. Thin absorbers
Horst, fontana, basilico, hansen adams

Interaction of charged particles

Real detector (limited granularity) can not measure $\langle dE/dx \rangle$!

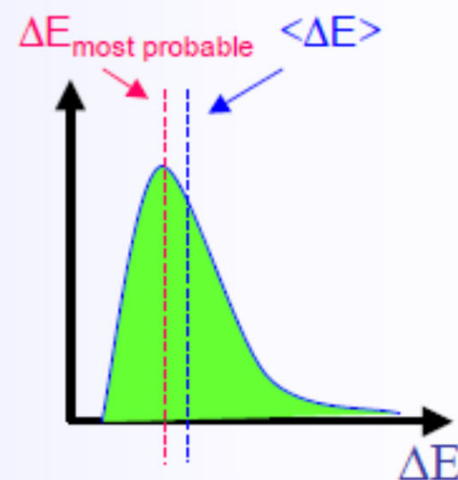
It measures the energy ΔE deposited in a layer of finite thickness δx .

For thin layers or low density materials:

→ Few collisions, some with high energy transfer.



→ Energy loss distributions show large fluctuations towards high losses: "Landau tails"

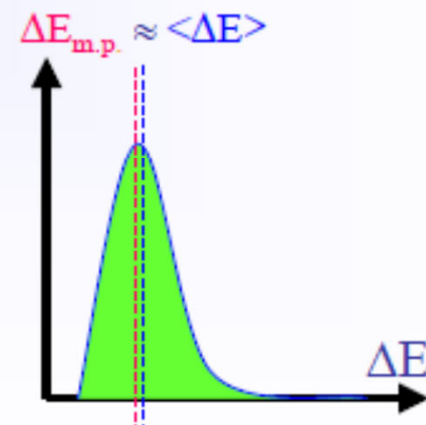
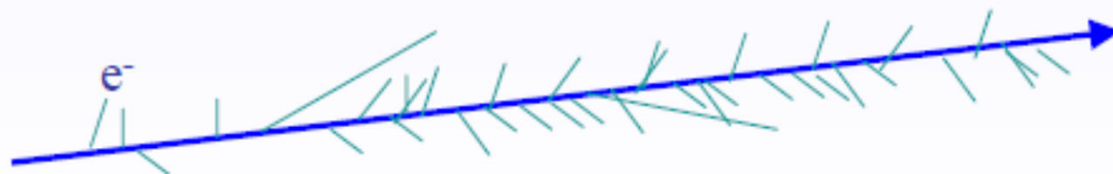


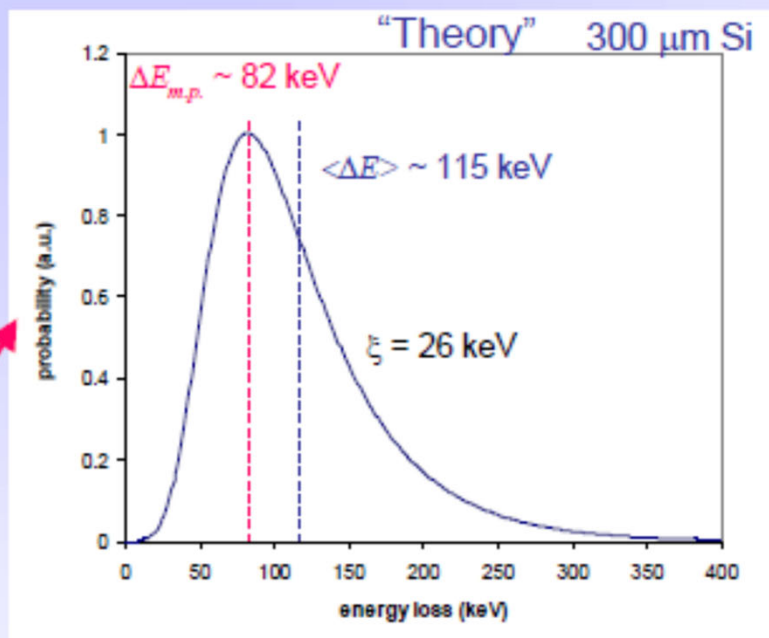
Example: Si sensor: 300 μm thick. $\Delta E_{\text{m.p.}} \sim 82 \text{ keV}$ $\langle \Delta E \rangle \sim 115 \text{ keV}$

For thick layers and high density materials:

→ Many collisions.

→ Central Limit Theorem → Gaussian shaped distributions.



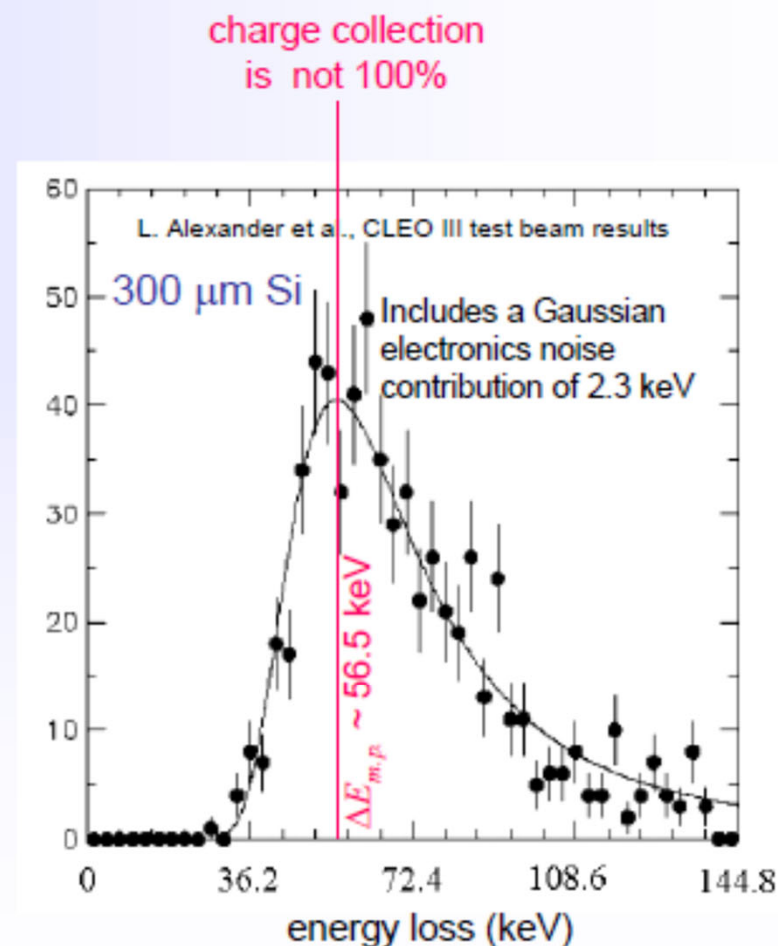


Landau's theory J. Phys (USSR) 8, 201 (1944)

$$f(x, \Delta E) = \frac{1}{\xi} \Omega(\lambda) \quad \Omega(\lambda) \approx \frac{1}{\sqrt{2\pi}} \exp\left\{-\frac{1}{2}(\lambda + e^{-\lambda})\right\}$$

$$\lambda = \frac{\Delta E - \Delta E_{m.p.}}{\xi}$$

$$\xi = \frac{2\pi N e^4 Z}{m_e v^2 A} x \quad x (300 \mu\text{m Si}) = 69 \text{ mg/cm}^2$$



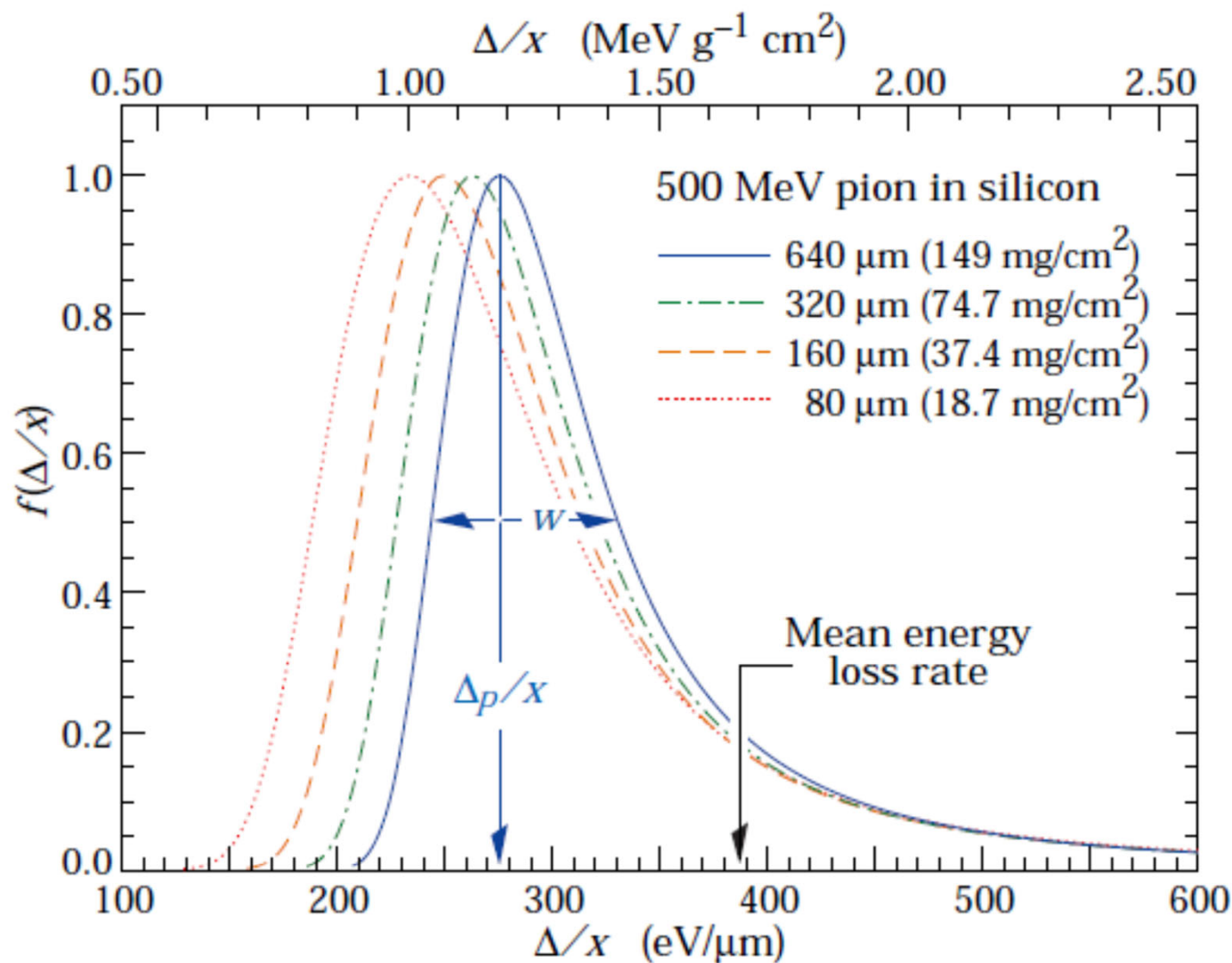


Figure 27.7: Straggling functions in silicon for 500 MeV pions, normalized to unity at the most probable value δ_p/x . The width w is the full width at half maximum.

fluttuazioni che sono descritte dalla distribuzione

Landau :

$$L(\lambda) = \frac{1}{(\sqrt{2\pi})} \exp\left(\frac{-1}{2}(\lambda + e^{(-\lambda)})\right)$$

- $\lambda = \frac{(\Delta E - \Delta E_m)}{(\zeta)}$
- $\zeta = 2\pi N_0 r_e^2 m_e z^2 c^2 \frac{Z}{A} \frac{1}{(\beta^2)} \rho x$

La grande fluttuazione nella perdita di energia tra un evento ed un altro condiziona la risoluzione energetica dei rivelatori sottili .

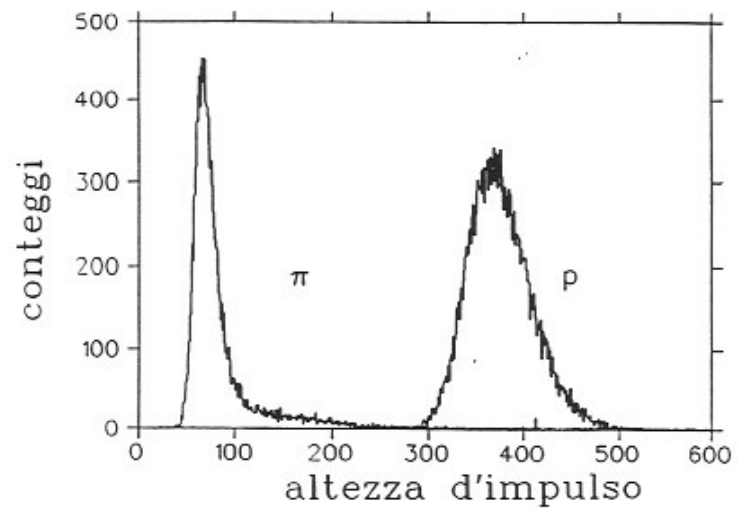


Fig.5.6- Altezza d'impulso di π^+ , p in $\Delta E1$ per $p=400$ MeV/c.

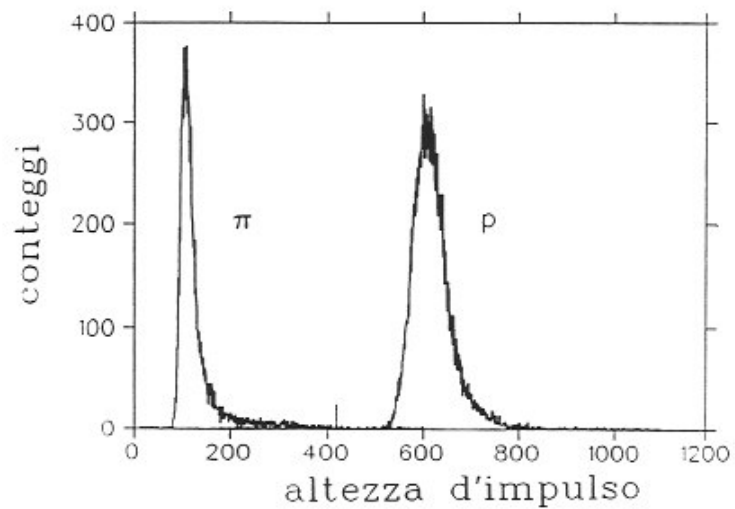


Fig.5.7- Altezza d'impulso di π^+ , p in $\Delta E2$ per $p=400$ MeV/c.

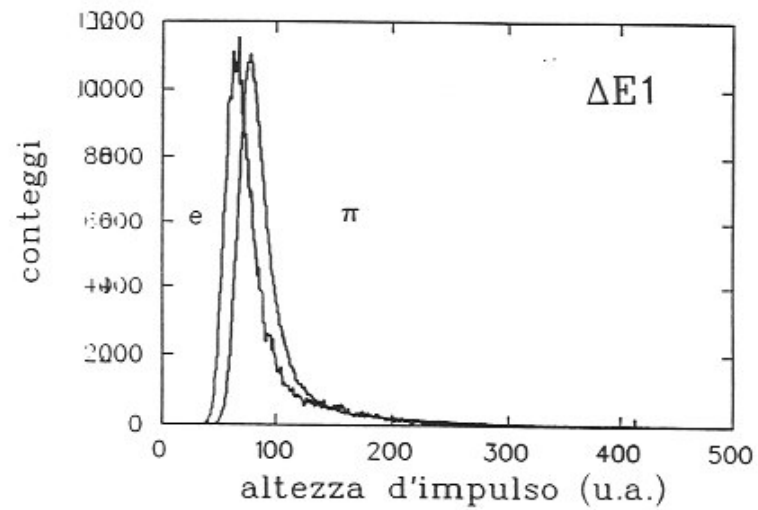


Fig.5.10- Altezza d'impulso di $e^+ \pi^+$ in $\Delta E1$ per $p=240 \text{ MeV}/c$.

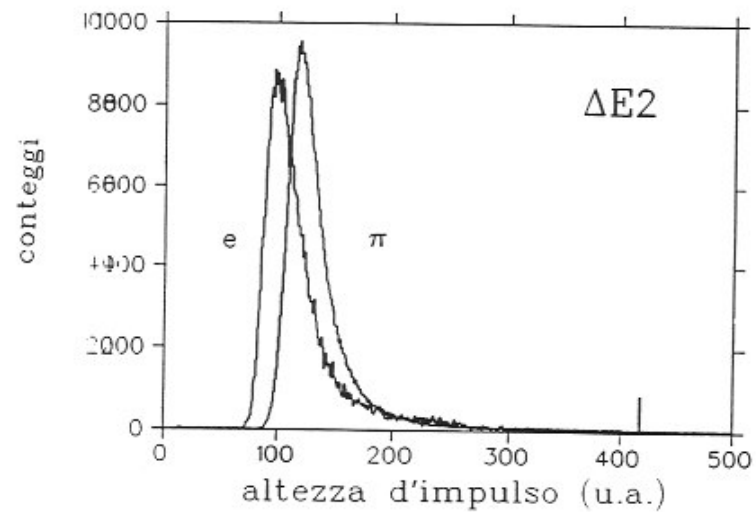
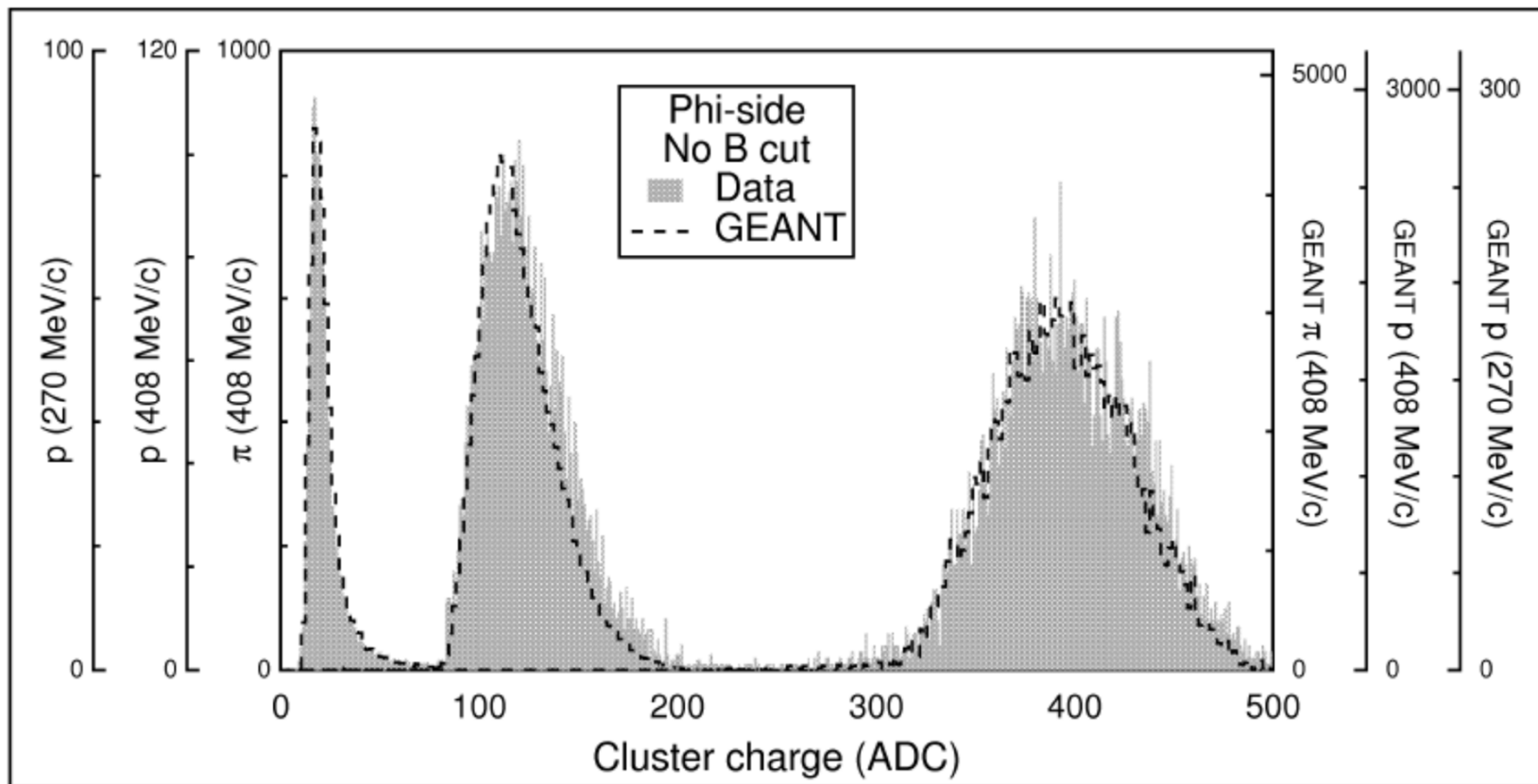
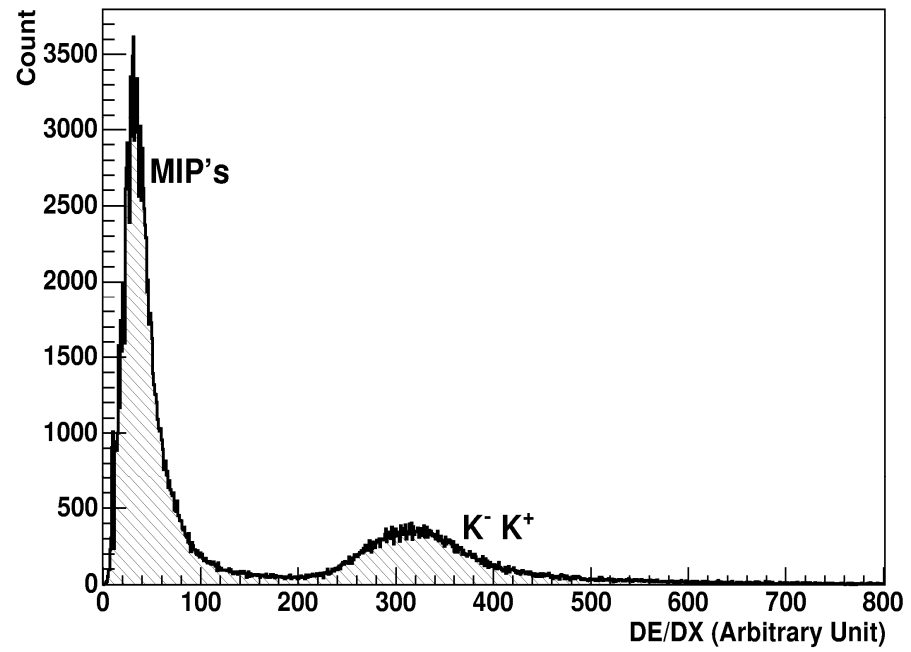
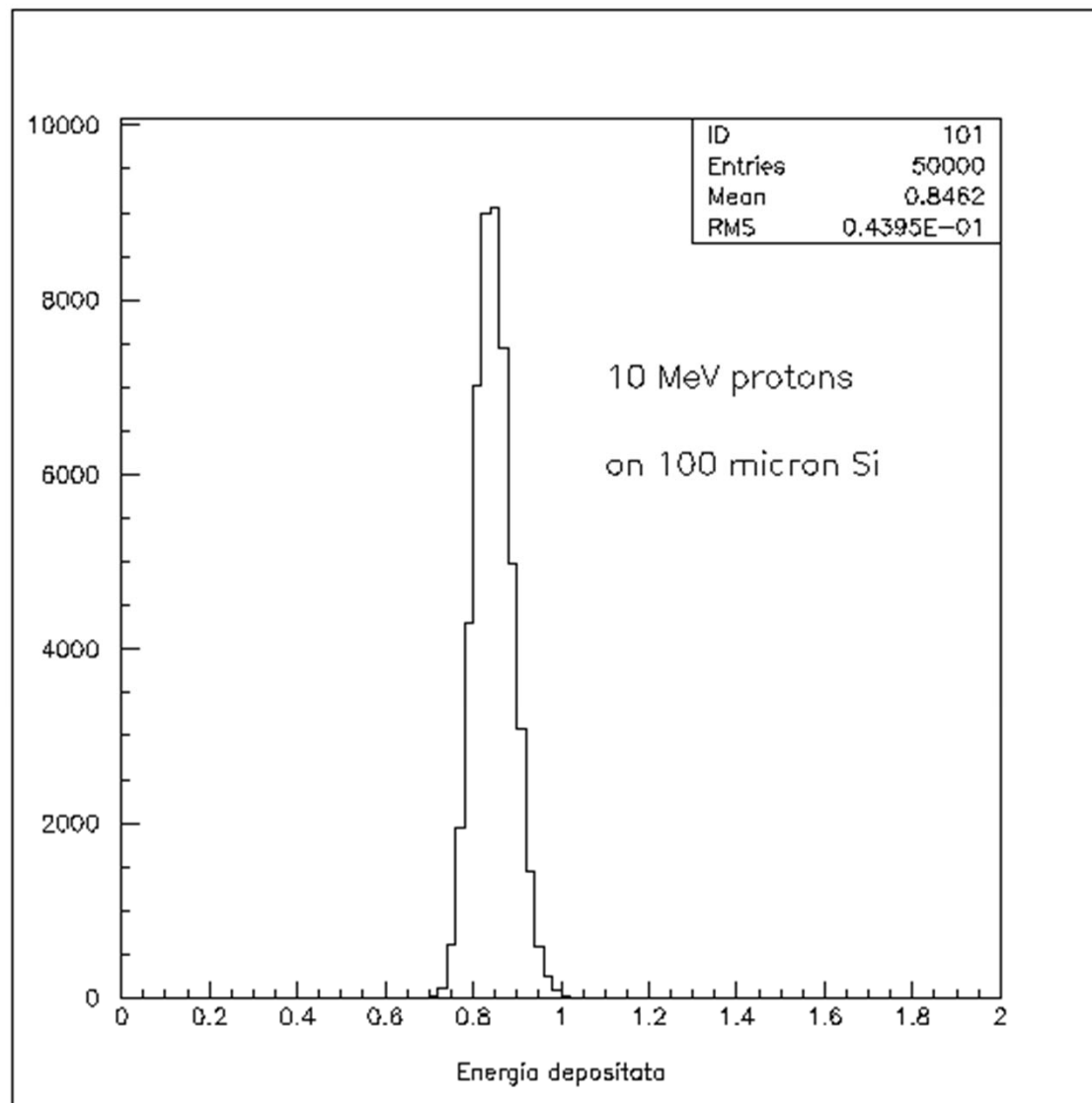
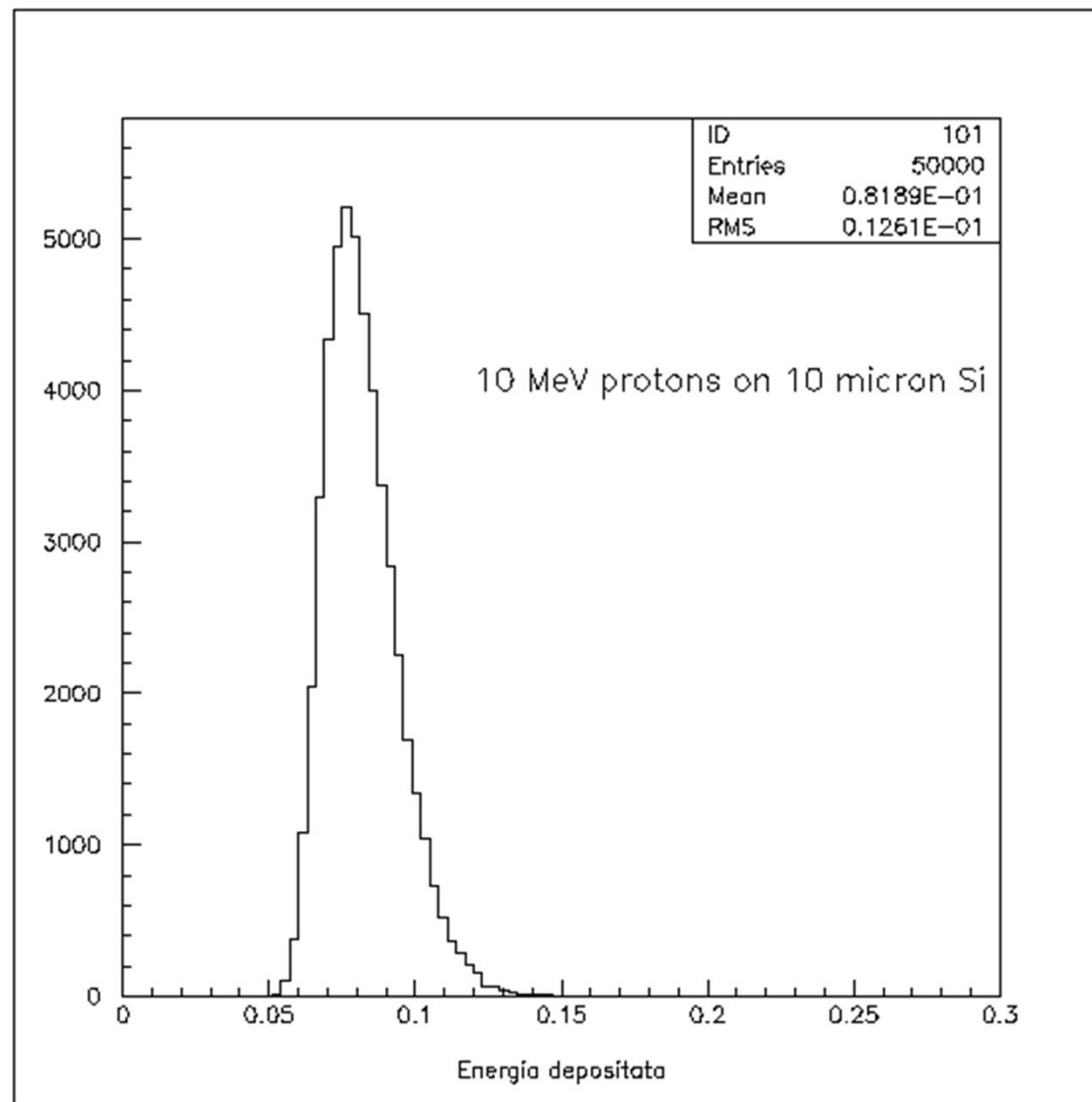


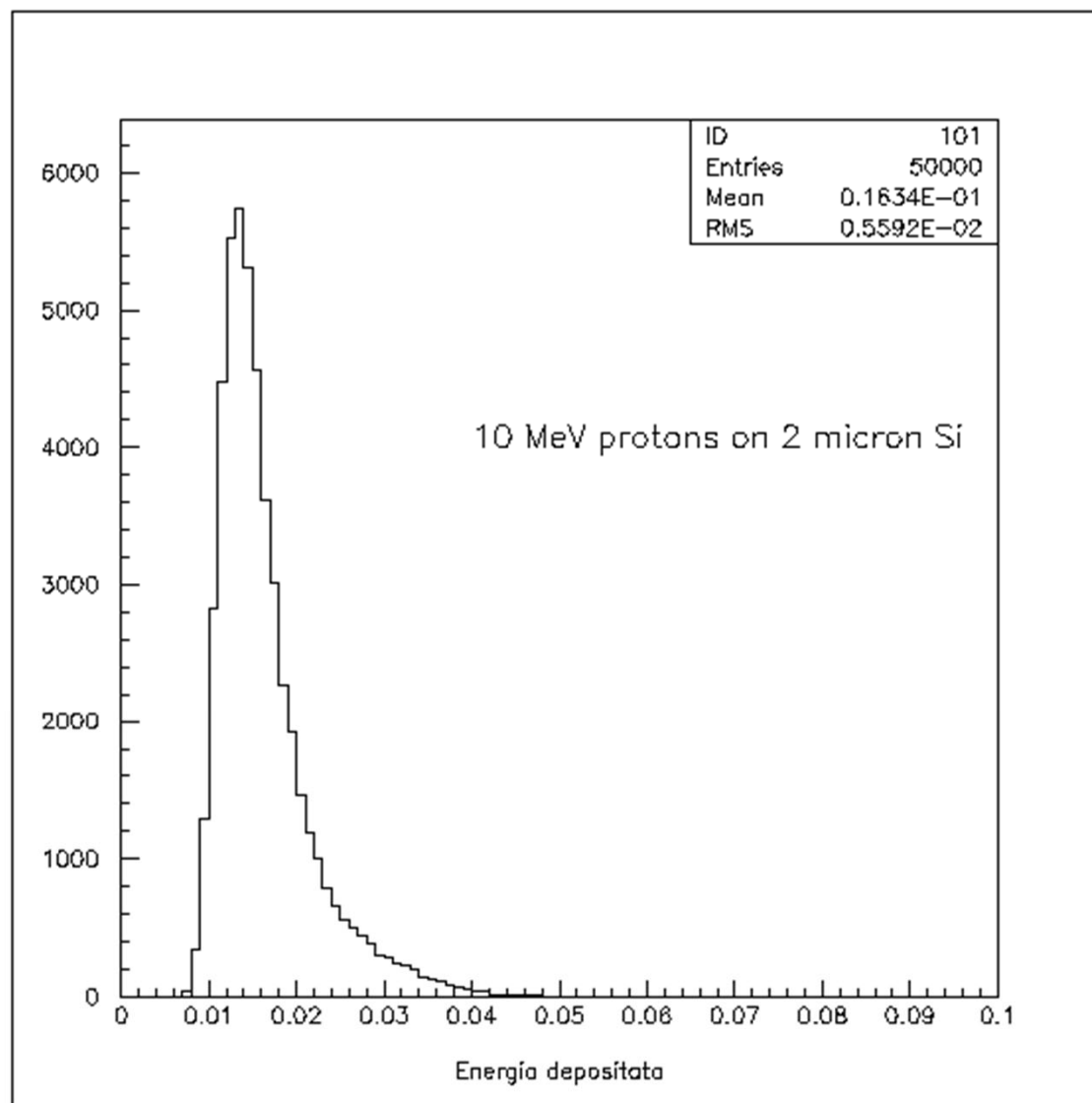
Fig.5.11- Altezza d'impulso di $e^+ \pi^+$ in $\Delta E2$ per $p=240 \text{ MeV}/c$.











tions

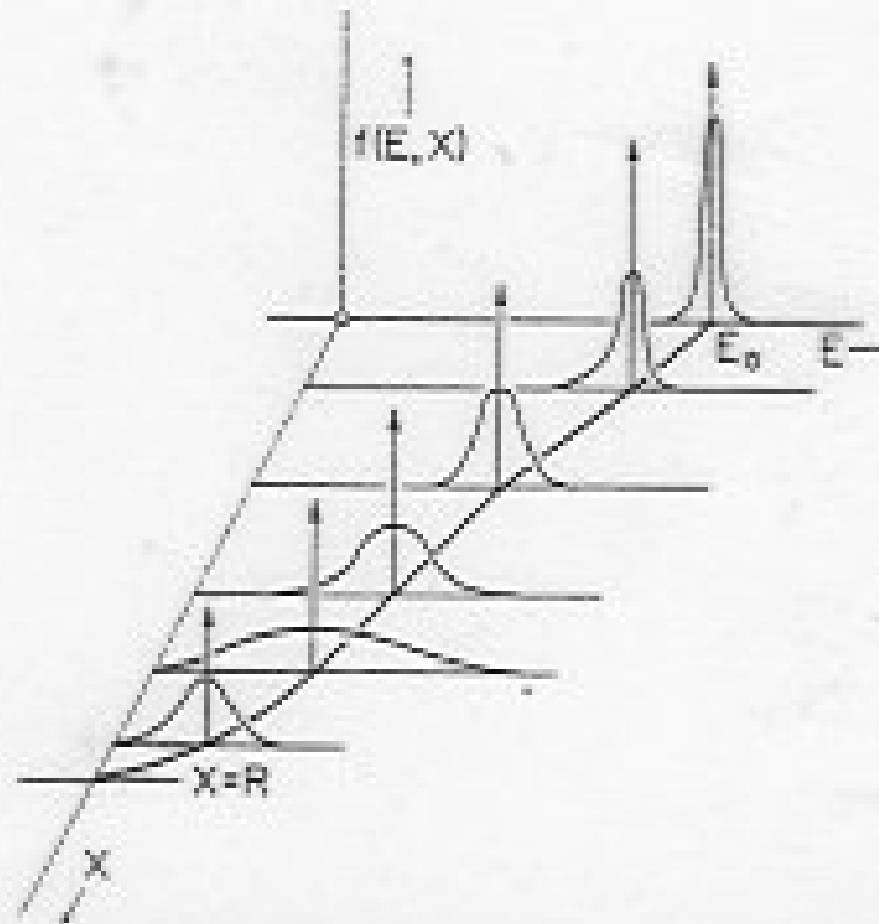


Figure 2.4 Plots of energy distribution of a beam of initially monoenergetic charged particles at various penetration distances. E is the particle energy and X is the distance along the track. (From Wilken and Fritz.³)

<http://www.nist.gov/pml/data/star/index.cfm>